THE ASTROPHYSICAL JOURNAL, 357:573–581, 1990 July 10

A NEW THEORETICAL CALIBRATION OF THE RELATION BETWEEN MASS-LOSS RATE AND Hα EMISSION FOR O STAR WINDS

J. E. DREW
Department of Astrophysics, Nuclear Physics Laboratory
Received 1989 October 13; accepted 1990 January 9

ABSTRACT

Luminosities of O star winds in H I Hα have been calculated from a series of wind ionization models based on the dynamical structure predicted by time-independent radiation-driven wind theory (Friend and Abbott; Pauldrach, Puls, and Kudritzki). The models span the entire range in effective temperature and luminosity falling within the O spectral class. A number of different velocity laws are considered. Best-fit relations involving $L(\mathrm{H}\alpha)$, $\dot{M}$, v_∞, and the stellar radius, R, are obtained for each velocity law.

Mass-loss rates obtained from observed values of $L(\mathrm{H}\alpha)$ using the new fits are compared with mass-loss rates for the same stars derived from radio flux measurements. The former are found to be, on average, about 2 times larger than the latter when the theoretically preferred $\beta = 0.7$ velocity law is assumed. Better agreement is achieved when a much more slowly accelerating $\beta = 1.5$ velocity law is used instead. Confirmation of this is obtained in a separate comparison with mass-loss rates derived semiempirically from H I Hα by Leitherer. It is suggested that this result may be evidence of enhanced Hα emission from the inner, accelerating portion of these winds, where the onset of wind instability gives rise to density inhomogeneities.

Subject headings: stars: early-type — stars: mass loss — stars: winds

I. INTRODUCTION

A major aim in studying the winds of hot stars is to find reliable methods for deriving mass-loss rates from observations of individual stars. This has to be done in order to quantify the effect of what is known to be substantial mass loss upon the evolution and lifetime of the most massive stars.

There are a number of different techniques available for determining O star mass-loss rates. One of these, based upon measurement of wind Hα emission, is the central concern of this study. The calibration of $\dot{M}$ against $L(\mathrm{H}\alpha)$, the wind luminosity in the H I Hα line, that has long been in use was derived by Klein and Castor (1978, hereafter KC). This has recently been updated by Leitherer (1988). In Leitherer's fit relating $\dot{M}$ and $L(\mathrm{H}\alpha)$, there is an adjustable parameter, I, whose value is fixed by requiring that Garmany and Conti's (1984) dependence of $\dot{M}$ upon bolometric luminosity is recovered for a large sample of OB stars. In this sense, the fit is semi-empirical and may be regarded as having been normalized to the ultraviolet mass-loss rates determined by Garmany and Conti (1984) and Garmany *et al.* (1981). Leitherer argues that the adjustable parameter, I, depends only on the wind velocity law and that the value he obtains is consistent with the predictions of time-independent theory (Friend and Abbott 1986; Pauldrach, Puls, and Kudritzki 1986).

In §§ II and III of this paper an alternative calibration of mass-loss rate in terms of Hα luminosity is presented. It is derived entirely theoretically by fitting the results of a new and extensive set of thermal and statistical equilibrium models of O star winds (Drew 1989, hereafter Paper I). These models depart from those of KC and other more recent publications in that the influence of heavy element spectral lines upon the thermal equilibrium is taken into account for the first time. This slightly modifies the predicted Hα emissivity by lowering the predicted wind temperatures (at two stellar radii, the new models yield $T_e \sim 0.6T_{\mathrm{eff}}$ rather than $T_e \sim 0.9T_{\mathrm{eff}}$). The adopted wind mass-loss rates used in the models are in accordance with the observationally based L_{bol}-$\dot{M}$ relation (Barlow 1985; Garmany and Conti 1984). For each set of stellar parameters and mass-loss rate, a variety of velocity laws are considered (including those consistent with time-independent radiation-driven wind theory). The dependence of $L(\mathrm{H}\alpha)$ upon $\dot{M}$ is derived directly from the models without any renormalization designed to ensure agreement with existing $\dot{M}$ determinations. In contradiction to Leitherer's (1988) conclusion, it is found that there are difficulties with the theoretically preferred velocity laws.

It is already clear that time-independent radiation-driven wind theory fails in certain respects. It is unable to explain either the weak X-ray emission from O stars detected by the *Einstein Observatory* (see the review by Cassinelli 1985) or the widespread occurrence of O VI λ1036 absorption in O star spectra (Snow and Morton 1976). These phenomena have encouraged the view that instabilities inherent in the wind driving mechanism may steepen into shocks as wind material is accelerated up to terminal velocity (Lucy 1982; Owocki, Castor, and Rybicki 1988). Such shocks would give rise to density perturbations that in turn can produce a number of other important effects. It shall be argued that these instabilities do in fact interfere with the $\dot{M}$-$L(\mathrm{H}\alpha)$ calibration derived on the basis of time-independent theory.

The theoretical $\dot{M}$-$L(\mathrm{H}\alpha)$ calibration is tested here primarily by comparing mass-loss rates deduced from H I Hα luminosities with mass-loss rates based on radio flux measurements. It has long been the consensus that radio $\dot{M}$ determinations are the best available. This is because in many instances the measured radio flux from an O star can be interpreted as being due to free-free emission in the wind, well away from the stellar surface, where we can be sure that the flow has reached terminal velocity (Wright and Barlow 1975; Panagia and Felli 1975). The observed radio flux is thus independent of the details of the wind acceleration (including the possible formation of shocks in the inner wind) and is only very weakly dependent upon the wind's ionization state and temperature: the main sensitivity is to the wind density at large radii and hence to the ratio $\dot{M}/v_\infty$.

Unfortunately, only a small number of the most luminous O stars are detectable at radio wavelengths (and some of those have been found to be non-thermal emitters thus preventing a mass-loss rate determination). So only a limited comparison is possible. This is described in § IV. The results of this comparison suggest that there is a systematic discrepancy between mass-loss rates derived using the theoretical $\dot{M}$-L(Hα) calibration for the preferred $\beta = 0.7$ velocity law and the radio determinations. Better agreement between the two methods is achieved when the Hα method assumes a $\beta = 1.5$ velocity law. In § V, confirmation of this result is sought by comparing the mass-loss rates predicted by the theoretical L(Hα) calibration with those obtained by Leitherer (1988). The significance of the results obtained is discussed in § VI.

II. THE CALCULATION OF H I Hα LUMINOSITIES

At the same time as the wind structure models described in Paper I were computed, Hα luminosities were obtained by numerical integration of an expression taken from KC for the net observable Hα emission per unit volume, $\epsilon(r)$. This may be written:

$$\epsilon(r) = h\nu_0\{[\beta(r) - \beta_c(r)]N_3(r)A_{32} - \beta_c(r)[N_2(r)B_{23} - N_3(r)B_{32}]I_{c,\nu_0}\} . \quad (1)$$

The quantities appearing here are defined as follows: ν_0 is the rest frequency of Hα emission; $N_2(r)$ and $N_3(r)$ are the number densities of neutral hydrogen atoms in the $n = 2$ and $n = 3$ excited states, respectively, at radius r; $\beta(r)$ is the local escape probability for Hα photons calculated using the Sobolev approximation as formulated by Castor (1970); $\beta_c(r)$ is the probability that an Hα photon emitted at radius r will escape into the solid angle occupied by the stellar core; A_{32}, B_{32}, and B_{23} are the Einstein coefficients for the Hα transition. The number densities, N_2 and N_3, and the escape probabilities, β and β_c, are calculated as functions of radius within the wind structure models presented in Paper I. The first term inside the braces in equation (1) is an emission term corrected for local line opacity and for photons lost as a result of back-scattering into the stellar core. The second term describes absorption in the line of the incident stellar continuum intensity, I_{c,ν_0}.

The integrated luminosity in the Hα line is given by

$$L(\mathrm{H}\alpha) = \int_R^\infty 4\pi r^2 \epsilon(r) dr , \quad (2)$$

in which R is the photospheric radius. Since a very fine radial mesh was used in the model calculations (typically in excess of 100 points per model), sufficient accuracy in the evaluation of equation (2) could be achieved by replacing the integration by a summation.

There are limitations to the use of equation (1) in evaluating net line luminosities. The expression requires that the Sobolev approximation is appropriate and that a plausible distinction exists between a continuum-emitting core and a surrounding envelope, optically thin in the continuum, in which the line of interest forms. In the case of Hα formation in O star winds, these requirements are satisfied as long as the velocity law is not too gradual ($\beta \lesssim 2$, see eq. [4]) and the mass-loss rate, not too high ($\dot{M} \lesssim 10^{-5}\ M_\odot$). Another problem that can arise is that absorption may be unduly exaggerated at small expansion velocities. This is because the Sobolev approximation does not allow for spatial diffusion of photons in regions of very high optical depth. This may not be too severe a difficulty in this case because the lower level of the Hα transition is an excited state. It is unlikely that the H I $n = 2$ population is ever so large in O star winds that the intrinsic line profile can develop significant coherently scattering damping wings.

The neglect of an underlying photospheric absorption profile in equation (1) is a relatively minor issue from the point of view of predicting wind Hα emission. This is so because Hα is formed primarily by recombination. However, from the practical point of view of deriving L(Hα) from observation, the neglect of photospheric absorption does present a serious problem in that a very uncertain, and sometimes large, correction for its effect may have to be applied to observed Hα profiles. This is particularly tricky at the lowest effective temperatures considered ($T_{\mathrm{eff}} \lesssim 30{,}000$ K), where wind emission and photospheric absorption become comparable. This is the main reason, apart from the range of stellar parameters actually modeled, why the fits derived here cannot be safely applied to B stars. L(Hα) has been calculated for a large number of O star wind models spanning the full range in both effective temperature and luminosity class. The input parameters are listed in Table 1. In each model, the mass-loss rate was chosen to agree with the following observationally based relation between $\dot{M}$ and bolometric stellar luminosity:

$$\dot{M} = 7.4 \times 10^{-8}(L/10^5\ L_\odot)^{1.72}\ M_\odot\ \mathrm{yr}^{-1} . \quad (3)$$

This was derived in a review by Barlow (1985) from ultraviolet mass-loss rates published by Garmany *et al.* (1981) and Garmany and Conti (1984) and radio mass-loss rates given by Abbott (1985). The conventional form of velocity law is used:

$$v(r) = v_R + (v_\infty - v_R)(1 - R/r)^\beta . \quad (4)$$

Time-independent radiation-driven wind theory suggests values for the index, β, in the range $0.6 \lesssim \beta \lesssim 1.0$ (Friend and Castor 1983; Friend and Abbott 1986; Pauldrach, Puls, and Kudritzki 1986). Infrared observations of OB supergiants have been interpreted by Bertout *et al.* (1985) as being consistent with a range in β extending to somewhat larger values ($0.6 \leq \beta \leq 2.0$). Since β is so uncertain or may indeed vary from star to star and because L(Hα) is sensitive to it, all the models listed in Table 1 have been calculated for more than one value of β. The supergiant sequence of models has received the most exhaustive treatment in this respect because their stronger Hα emission is most easily measured. In every case, the wind speed v_R at the photospheric radius is set at 10 km s^{-1}, a value comparable with the sound speed. Except where the wind Hα luminosity is teetering on the limit of detectability [L(Hα) $\sim 0.1\ L_\odot$], the dependence on v_R is very weak; for L(Hα) $\sim L_\odot$, halving or doubling the chosen value of v_R was found to change L(Hα) by at most a few percent. Most of the terminal velocities given in Table 1 were chosen such that $v_\infty \approx 3v_{\mathrm{esc}}$, where v_{esc} is the escape velocity at the stellar surface. For three spectral types, additional models were calculated for terminal velocities both larger and smaller than $3v_{\mathrm{esc}}$. This was done just to diversify the model set a little. The surface gravities (log g), also given in Table 1, were mostly chosen to be the same as those included by Mihalas (1972) in his grid of non–LTE model atmospheres. This is because the stellar continuum fluxes, used in the wind equilibrium calculations, were taken from Mihalas (1972).

TABLE 1

MODEL STELLAR AND WIND PARAMETERS

Approximate Spectral Subtype and Luminosity Class	T_* (K)	L_{bol} ($10^5 L_\odot$)	R ($R_\odot$)	log g	$\dot{M}$ ($M_\odot$ yr^{-1})	v_∞ (km s^{-1})
			Supergiants			
O3 I	50,000	20	19	4.0	1.2×10^{-5}	2400
O4 I	45,000	13	19	4.0	6.0×10^{-6}	2900
O5 I	40,000	12	23	3.5	5.5×10^{-6}	1500
						2300
						3100
O6.5 I	37,500	9.4	23	3.5	3.5×10^{-6}	2300
O7.5 I	35,000	6.3	22	3.3	1.8×10^{-6}	1800
O9 I	32,500	4.1	20	3.3	8.3×10^{-7}	1400
						1800
						2400
O9.5 I	30,000	3.0	20	3.0	4.8×10^{-7}	1800
			Giants			
O6 III	40,000	4.8	14	4.0	1.1×10^{-6}	2900
O6.5 III	37,500	3.7	14	4.0	7.0×10^{-7}	2900
O7.5 III	35,000	2.3	13	4.0	3.0×10^{-7}	2900
			Main Sequence			
	55,000	11	11	4.0	4.5×10^{-6}	2500
O3 V	50,000	7.5	11	4.0	2.3×10^{-6}	2300
						3000
						3500
O5 V	45,000	4.9	11	4.0	1.1×10^{-6}	3200
O6.5 V	40,000	2.3	10	4.0	3.2×10^{-7}	3200

All calculated values of $L(\mathrm{H}\alpha)$ (expressed in units of $L_\odot$) are listed in Table 2. Also quoted are the equivalent widths in Å to which these luminosities can be expected to correspond. The results presented are limited to those where $L(\mathrm{H}\alpha)$ was found to be $\gtrsim 0.1\ L_\odot$. Weaker calculated Hα luminosities are not to be trusted because of the sensitivity to v_R.

III. FITS TO $L(\mathrm{H}\alpha)$ IN TERMS OF $\dot{M}$, VELOCITY LAW, AND STELLAR RADIUS

The calculated wind Hα emission can now be used to obtain a fit relating its magnitude to the relevant quantities. These appear to be $\dot{M}$, v_∞, the velocity law index, β, and the stellar radius, R. No evidence for a clear-cut dependence on stellar effective temperature was found. A fit to the total normalized luminosity in the line, $L(\mathrm{H}\alpha)/L_\odot$, is considered in preference to one to the line equivalent width. The main reason for this is that $L(\mathrm{H}\alpha)$ depends primarily upon wind parameters and shows only slight sensitivity to photospheric properties, whereas the line equivalent width is strongly dependent on both. It is, of course, impossible to avoid some dependence on adopted stellar parameters because the observations are usually spectroscopic, rather than spectrophotometric, and because a correction often has to be made for underlying photospheric absorption.

Values of $L(\mathrm{H}\alpha)$ derived from observation depend explicitly on D, the stellar distance. This turns out to be an advantage when it comes to comparing radio mass loss rates with Hα mass-loss rates, since the former also depend on D and, indeed, the power of the dependence is much the same in both methods (see § IV). The useful consequence of this is that the comparison is effectively distance independent. The dependence on D becomes a drawback in determining $\dot{M}$ for particular stars, but again some dependence would be unavoidable even if $\dot{M}$ could be determined from the Hα equivalent width instead because, then, an estimate of the star's bolometric luminosity would be needed. Taking the results obtained for each velocity law separately, the values of $L(\mathrm{H}\alpha)/L_\odot$ given in Table 2 have been fit to expressions of the form

$$L(\mathrm{H}\alpha)/L_\odot = a_1 \dot{M}_{-6}^{a_2} v_{\infty,3}^{-a_3}\,, \tag{5}$$

and

$$L(\mathrm{H}\alpha)/L_\odot = b_1 \dot{M}_{-6}^{b_2} v_{\infty,3}^{-b_3} R^{b_4}\,, \tag{6}$$

in which $\dot{M}_{-6}$ is the mass-loss-rate in units of $10^{-6}\ M_\odot$ yr^{-1}, $v_{\infty,3}$ is the terminal velocity given in 1000 km s^{-1}, and R is the photospheric radius in units of $R_\odot$. For each velocity law (choice of β), there are thus three or four constants (a_i and b_i) to determine by least-squares fitting. The values obtained are given in Table 3.

The reason for trying fits with and without a dependence on stellar radius is to establish whether it is really necessary to include this quantity. Some dependence might be expected because the wind emission measure and optical depth both scale as $1/R$. However, since increased optical depth and an increased emission measure effect the Hα luminosity in opposite senses, it might also be argued that at least some cancellation occurs and hence the dependence on R is very weak. That the dependence on R is significantly weaker than the dependence on $\dot{M}$ and v_∞ is confirmed by comparing the best-fit values of b_4 with those of b_2 and b_3 given in Table 3: $L(\mathrm{H}\alpha)/L_\odot$ shows no more than a square-root dependence on R, while the power of the dependence on $\dot{M}$ and $1/v_\infty$ is of order unity or greater.

To see if it is possible to get by with fits leaving R out altogether, it is necessary to investigate the residuals between each

TABLE 2

CALCULATED H I Hα LUMINOSITIES AND EQUIVALENT WIDTHS

T_* (K)	$\dot{M}$ ($M_\odot$ yr^{-1})	v_∞ (km s^{-1})	$\beta = 0.7$ $L(\mathrm{H}\alpha)/L_\odot$	$\beta = 0.7$ W (Å)	$\beta = 1.0$ $L(\mathrm{H}\alpha)/L_\odot$	$\beta = 1.0$ W (Å)	$\beta = 1.5$ $L(\mathrm{H}\alpha)/L_\odot$	$\beta = 1.5$ W (Å)	$\beta = 2.0$ $L(\mathrm{H}\alpha)/L_\odot$	$\beta = 2.0$ W (Å)
					Supergiants					
50,000......	1.2×10^{-5}	2400	17.14	8.0	22.71	10.6	32.14	15.0	41.02	19.2
45,000......	6.0×10^{-6}	2900	4.83	2.4	7.42	3.7	12.07	6.1	16.72	8.5
40,000......	5.5×10^{-6}	1500	10.06	4.1	13.82	5.5	20.36	8.1		
		2300	5.28	2.1	8.02	3.2	13.04	5.2	18.08	5.2
		3100	3.32	1.3	5.57	2.2	9.77	3.9		
37,500......	3.5×10^{-6}	2300	2.95	1.3	4.83	2.1	8.44	3.6	12.28	3.5
35,000......	1.8×10^{-6}	1800	1.59	0.9	2.64	1.4	4.73	2.5	6.87	3.6
32,500......	8.3×10^{-7}	1400	0.88	0.6	1.52	1.1	2.80	1.9		
		1800	0.59	0.4	1.12	0.8	2.18	1.5	3.32	2.2
		2400	0.37	0.3	0.77	0.5	1.67	1.1		
30,000......	4.8×10^{-7}	1800	0.26	0.2	0.50	0.4	1.05	0.8	1.64	1.3
					Giants					
40,000......	1.1×10^{-6}	2900	0.36	0.3	0.78	0.7	1.63	1.5	...	...
37,500......	7.0×10^{-7}	2900	0.20	0.2	0.48	0.5	1.07	1.2	...	...
35,000......	3.0×10^{-7}	2900	0.07	0.1	0.17	0.2	0.44	0.6	...	...
					Main Sequence					
55,000......	4.5×10^{-6}	2500	3.42	3.8	4.76	5.3	7.13	7.9	...	...
50,000......	2.3×10^{-6}	2300	1.45	1.8	2.27	2.8	3.58	4.4	...	...
		3000	0.91	1.3	1.58	1.9	2.74	3.4	...	...
		3500	0.70	1.0	1.29	1.6	2.33	2.9	...	...
45,000......	1.1×10^{-6}	3200	0.26	0.4	0.56	0.8	1.15	1.6	...	...
40,000......	3.2×10^{-7}	3200	0.04	0.1	0.11	0.2	0.29	0.5	...	...

of the types of fit to $L(\mathrm{H}\alpha)/L_\odot$ (eqs. [5] and [6]) and the model values in Table 2. These are plotted in Figures 1 and 2, which show that the fits involving R as well as $\dot{M}$ and v_∞ do represent an improvement on those without. The main improvement is that the supergiant and dwarf results mingle better when R is included in the fit (Fig. 2) than when it is not (Fig. 1). Indeed, the noticeable separation between these luminosity classes in Figure 1 suggests that a fit parameter has been missed out. Also, when R is included in the fits, there is a reduction in the rms residual from 0.12 down to 0.08.

Before going on to find out what sense these fits can make of observed estimates of $L(\mathrm{H}\alpha)$, it is of interest to consider the pattern of variation of $L(\mathrm{H}\alpha)$ that they imply. The fit parameters given in Table 3 show that the dependence of $L(\mathrm{H}\alpha)$ upon $\dot{M}$ and v_∞ is strongest in steeply accelerating winds (small β). This is associated with steeper acceleration bringing the wind closer to the limit of no absorption in which one would expect $L(\mathrm{H}\alpha) \propto \int n_e n_{\mathrm{H}^+}\, dV \propto (\dot{M}/v_\infty)^2$ (see the discussion of this point by KC). The weakening dependence upon R for faster velocity laws has the same origin. It is indicative of the occurrence of some absorption, even in relatively rapidly accelerated, low $\dot{M}$ winds, that the $(\dot{M}/v_\infty)^2$ dependence is not realized and that the power of the dependence on R is positive. If line opacity were negligible at all radii, the expected behavior of $L(\mathrm{H}\alpha)$ is the opposite in that it should decrease with increasing R in response to the falling emission measure ($\int n_e n_{\mathrm{H}^+}\, dV \propto 1/R$) and so be proportional to a negative power of R. It is consistent with the significant role attributed to absorption that b_4 is

TABLE 3

VALUES OF THE FIT PARAMETERS, a_i AND b_i, FOR DIFFERENT VELOCITY LAWS[a]

PARAMETER	β = 0.7	1.0	1.5	2.0
a_1	2.050	3.129	5.382	6.177
a_2	1.437	1.270	1.120	1.059
a_3	1.768	1.472	1.288	0.839
b_1	0.932	0.914	0.848	5.238
b_2	1.415	1.236	1.068	1.058
b_3	1.599	1.208	0.892	0.825
b_4	0.234	0.365	0.548	0.052

[a] See eqs. (5) and (6).

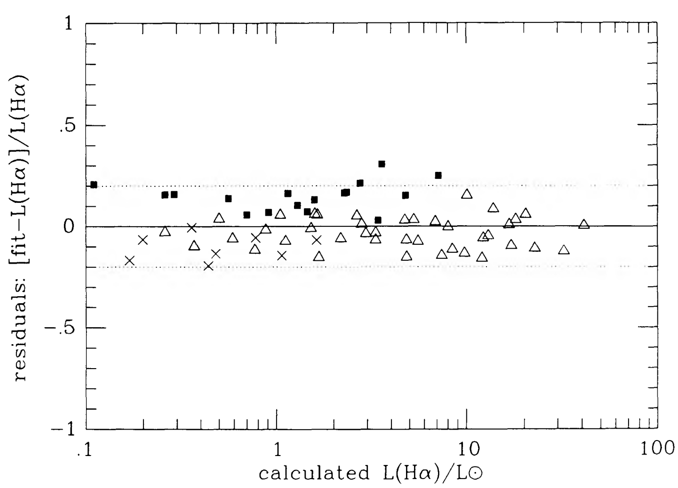

FIG. 1.—The residuals for the fits excluding R as a fit parameter (see eq [5]) plotted as a function of the calculated values of $L(\mathrm{H}\alpha)$ listed in Table 2. The supergiant residuals are plotted as triangles. The giant and main-sequence dwarf points are plotted as crosses and solid squares, respectively.

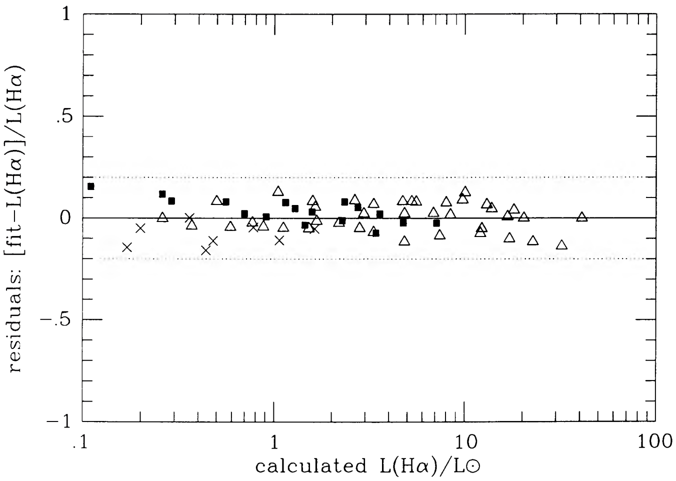

FIG. 2.—The residuals for the fits including R as a fit parameter (see eq. [6]) plotted as a function of the calculated values of $L(\mathrm{H}\alpha)$. Symbols have the same meaning as in Fig. 1.

larger for slower velocity laws (excepting $\beta = 2$, where the fit suffers from small number statistics), since the integrated wind optical depth is larger in more slowly accelerated winds.

IV. COMPARISON OF THE $\dot{M}$-$L(\mathrm{H}\alpha)$ CALIBRATION WITH RADIO MASS-LOSS RATE DETERMINATIONS

For the purpose of determining mass-loss rates from Hα observations, equation (6) can be rewritten in the more convenient form

$$\log \dot{M}_{-6} = \frac{1}{b_2} \log \left[\frac{L(\mathrm{H}\alpha)}{L_\odot}\right] + \frac{b_3}{b_2} \log v_{\infty,3} - \frac{b_4}{b_2} \log R - b_2 \log b_1 \,, \quad (7)$$

On substituting the fit parameters given in Table 3 for $\beta = 0.7$, 1.0, and 1.5, equation (7) becomes

$$\begin{aligned} \log \dot{M}_{-6} &= 0.707 \log [L(\mathrm{H}\alpha)/L_\odot] + 1.130 \log v_{\infty,3} \\ &\quad - 0.165 \log R + 0.022 \quad \beta = 0.7 \,, \\ &= 0.809 \log [L(\mathrm{H}\alpha)/L_\odot] + 0.977 \log v_{\infty,3} \\ &\quad - 0.296 \log R + 0.032 \quad \beta = 1.0 \,, \\ &= 0.936 \log [L(\mathrm{H}\alpha)/L_\odot] + 0.835 \log v_{\infty,3} \\ &\quad - 0.513 \log R + 0.067 \quad \beta = 1.5 \,. \end{aligned} \quad (8)$$

Of these velocity laws, the first for $\beta = 0.7$ is typical of the predictions of time-independent theory (Friend and Abbott 1986; Pauldrach, Puls, and Kudritzki 1986). All three are considered in order to establish how sensitive derived mass-loss rates are to the assumed velocity law.

Those O stars whose mass-loss rates have been derived from definite detections of radio emission are listed in Table 4. These estimates are taken from either Abbott (1985) or from Bieging, Abbott, and Churchwell (1989). For each star, there is reason to assume that the radio emission is thermal in origin, as it must be to provide a means of measuring the mass-loss rate. Cyg OB2 No. 9 is usually a nonthermal emitter, but it can be included here because its mass-loss rate has been determined from a radio observation obtained when the nonthermal component was absent. Strictly, one of the entries in Table 4, ε Ori (B0 Ia), should not have been included because its effective temperature (~26,000 K) lies below the modeled range (30,000 K ≤ T_{eff} ≤ 55,000 K). However, it is retained on the grounds that the winds of the earliest B0 supergiants are likely to follow the same trend as the O supergiants down to the effective temperature below which photospheric absorption in the H I Lyman continuum is strong enough to bring about a qualitative change in the character of the wind hydrogen ionization. In Mihalas's (1972) non–LTE model atmospheres, the Lyman discontinuity only becomes prominent for effective temperatures below 25,000 K. The more serious question concerning its inclusion in the sample, and also the inclusion of ζ Ori and α Cam, is the relatively strong Hα photospheric absorption. This is taken into account below in the error assessment.

All the terminal velocities quoted in Table 4 have been taken from the same references as the radio mass-loss rate estimates. This tactic is adopted in order to prevent uncertainties in the terminal velocities from significantly distorting the comparison between the two methods of mass-loss rate determination. All values of log $[L(\mathrm{H}\alpha)/L_\odot]$ and R are from Leitherer (1988, Table 1), who collected together observations of Hα equivalent widths and uniformly translated them into luminosity estimates. Of the stars listed in Table 4, only α Cam is not a member of a known cluster and thus lacks a reliable distance estimate. Hence, only in this case is it at all possible that errors in the distance, D, might influence the comparison between the radio and Hα methods. Indeed, it is important to note that the similarity in the dependence of $\dot{M}$ both upon D and v_∞ in the two methods (radio: $\dot{M} \propto D^{1.5} v_\infty$; Hα: $\dot{M} \propto D^{1.414} v_\infty{}^{1.13}$[$\beta$ = 0.7], $\dot{M} \propto D^{1.618} v_\infty{}^{0.835}$[$\beta$ = 1.5]), renders the ratio of the derived mass-loss rates effectively independent of both these quantities.

Using equation (8), mass-loss rates have been obtained from

TABLE 4

MASS-LOSS RATES DERIVED FROM RADIO FLUX DETECTIONS AND FROM Hα LUMINOSITIES FOR THE β = 0.7, 1.0, AND 1.5 VELOCITY LEVELS

Name	HD Number	Spectral Type	$\dot{M}$(radio) ($M_\odot$ yr^{-1})	Reference[a]	v_∞ (km s^{-1})	log $[L(\mathrm{H}\alpha)/L_\odot]$	$\dot{M}$(Hα) ($M_\odot$ yr^{-1}) β = 0.7	β = 1.0	β = 1.5
ζ Ori	37742	O9.7 Ib	2.3×10^{-6}	1	2300	0.87	6.2×10^{-6}	4.3×10^{-6}	2.5×10^{-6}
ε Ori	37128	B0 Ia	3.1×10^{-6}	1	2000	0.86	5.1×10^{-6}	3.6×10^{-6}	2.1×10^{-6}
ζ Pup	66811	O4f	5.0×10^{-6}	2	2400	1.02	9.3×10^{-6}	7.2×10^{-6}	5.1×10^{-6}
α Cam	30614	O9.5 Ia	5.4×10^{-6}	2	1890	1.03	6.6×10^{-6}	5.0×10^{-6}	3.2×10^{-6}
	151804	O8 Iaf	1.0×10^{-5}	2	2000	1.87	2.7×10^{-5}	2.5×10^{-5}	1.9×10^{-5}
Cyg OB2 No. 9	...	O5 If	1.9×10^{-5}	1	2650	1.67	2.7×10^{-5}	2.2×10^{-5}	1.6×10^{-5}
	152408	O8 Iafpe	2.5×10^{-5}	2	1800	2.12	3.6×10^{-5}	3.6×10^{-5}	3.2×10^{-5}

[a] References for radio $\dot{M}$ and v_∞ values: (1) Abbott 1985; (2) Bieging, Abbott, and Churchwell 1989.

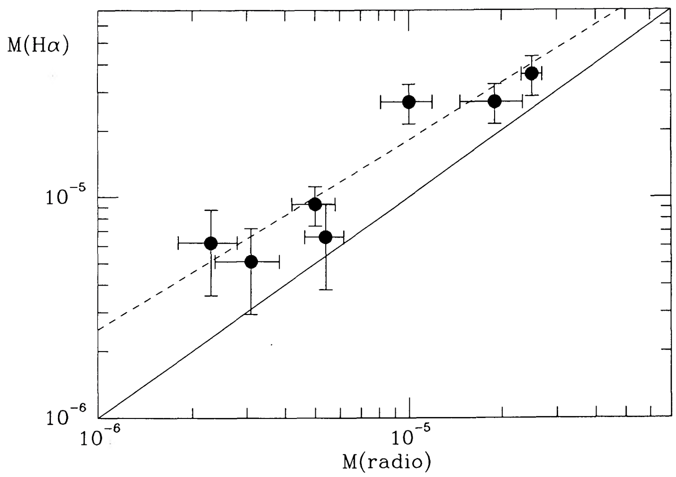

FIG. 3.—For the stars listed in Table 4, mass-loss rates derived from $L(\mathrm{H}\alpha)$ measurements assuming a $\beta = 0.7$ velocity law (see eq [8]) are shown plotted against the mass-loss rates derived from radio flux measurements. Error bars represent the uncertainty in the original flux determinations and the fitting error: errors associated with the stellar distances and wind terminal velocities are not included, since these propagate almost identically in the two methods. The best-fit power-law relation between the two sets of derived mass-loss rates is drawn as a dashed line. Along the solid line, the two mass-loss rates are equal.

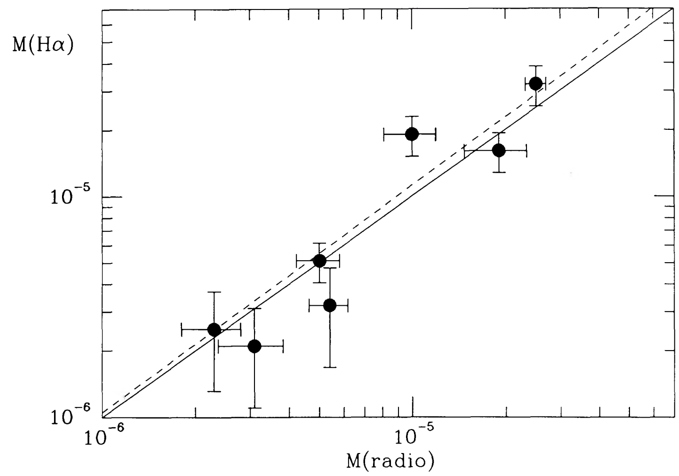

FIG. 5.—For the stars listed in Table 4, mass-loss rates derived from $L(\mathrm{H}\alpha)$ measurements assuming a $\beta = 1.5$ velocity law (see eq. [8]) are shown plotted against the mass-loss rates derived from radio flux measurements. Error bars represent the uncertainty in the original flux determinations and the fitting error. The formal best-fit power law relation between the two sets of derived mass-loss rates is drawn as a dashed line. In this case, the best-fit power law is statistically quite indistinguishable from equality between the two methods of $\dot{M}$ determination.

the values of log $[L(\mathrm{H}\alpha)/L_\odot]$ and v_∞ given in Table 4. The results for the $\beta = 0.7$, 1.0, and 1.5 velocity laws are plotted against the radio mass-loss rates in Figures 3, 4, and 5, respectively. It is immediately apparent from these results that the $L(\mathrm{H}\alpha)/L_\odot$ fit for the theoretically preferred $\beta = 0.7$ velocity law always yields an $\dot{M}$ estimate larger than that obtained from a radio flux measurement. On average, the scaling between the two is about a factor of 2. There is some improvement in the comparison when the $\beta = 1.0$ fit is adopted, but there is still a clear tendency apparent in the Hα method toward overestimating $\dot{M}$ (see Fig. 4). The agreement between the two methods of mass-loss rate determination is best when the $\beta = 1.5$ fit is used (Fig. 5).

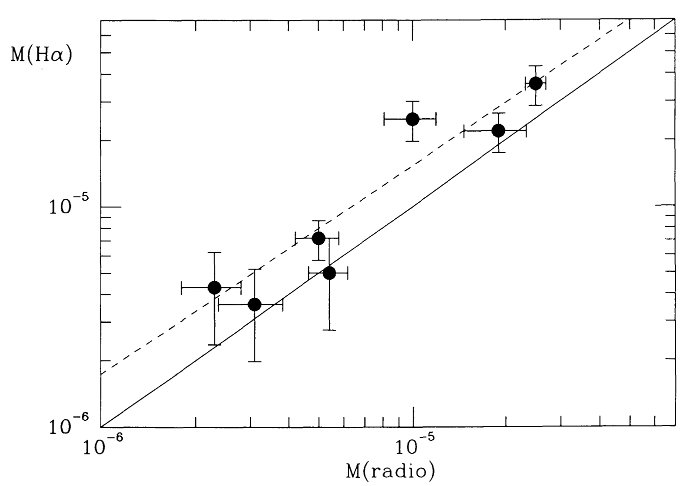

FIG. 4.—For the stars listed in Table 4, mass-loss rates derived from $L(\mathrm{H}\alpha)$ measurements assuming a $\beta = 1.0$ velocity law (see eq. [8]) are shown plotted against the mass-loss rates derived from radio flux measurements. Error bars represent the uncertainty in the original flux determinations and the fitting error. The formal best-fit power law relation between the two sets of derived mass-loss rates is drawn as a dashed line.

To aid in the interpretation of the comparison, errors in the derived mass-loss rates have been estimated individually for each star and are plotted in Figures 3, 4, and 5. The errors in the radio mass-loss rates are 0.75 times the published uncertainties in the 6 cm flux measurements ($\dot{M}$ is proportional to $[\mathrm{flux}]^{0.75}$). An uncertainty of 20% is attributed to the Hα calibration (allowing a fitting error and an uncertainty in the model Hα fluxes of 10% each). A further error of 30% is attributed to the correction for photospheric absorption in the observed Hα profiles of the coolest stars in Table 4 (ϵ Ori, ζ Ori, and α Cam). Since the uncertainties associated both with the adopted terminal velocities and with the assumed stellar distances introduce the same fractional error in both methods of $\dot{M}$ determination (as argued above), errors due to these factors can be neglected.

These error estimates can be used in obtaining a best-fit relation between the plotted radio and Hα mass-loss rates. At this point, it should be noted that there is considerable uncertainty over the evolutionary status of one of the stars in this small sample. Walborn (1982) indicated that HD 152408 may be regarded as either an Of star or as in transition to the Wolf-Rayet class: if it is is the latter, the characteristics of its photosphere and wind are probably not of the type to which the present Hα calibration can be applied. In view of this, the relatively small $\dot{M}$ errors obtained for HD 152408 were arbitrarily increased for the purposes of the fit calculations to be in line with the largest errors present in the sample. The derived best-fit relations are drawn as a dashed line in each of Figures 3, 4, and 5. The assumed functional form is linear in the log-log plane. The best-fit relations shown in Figures 3, 4, and 5 for each of the velocity laws, may be written:

$$\begin{aligned} \log \dot{M}(\mathrm{H}\alpha) &= 0.396 + 0.861 \log \dot{M}(\mathrm{radio}) \quad \beta = 0.7\,, \\ &= 0.239 + 0.947 \log \dot{M}(\mathrm{radio}) \quad \beta = 1.0\,, \\ &= 0.021 + 1.028 \log \dot{M}(\mathrm{radio}) \quad \beta = 1.5\,. \end{aligned} \tag{9}$$

Both the radio and Hα mass-loss rates are in units of $10^{-6}\ M_\odot\ \mathrm{yr}^{-1}$. The best-fit relation obtained for the $\beta = 1.5$ results is statistically indistinguishable from equality between the two methods.

V. COMPARISON OF THE THEORETICAL $\dot{M}$-L(Hα) CALIBRATION WITH THE SEMIEMPIRICAL METHOD OF LEITHERER (1988)

The conclusion of the previous section is at variance with Leitherer's (1988) finding that a $\beta \sim 0.7$ does give satisfactory results in his L(Hα)-$\dot{M}$ calibration for O stars. This divergence between the two calibrations must be explained. The main difference in the physics in the two prescriptions of O star wind Hα production arises in the role attributed to wind absorption. Leitherer decided to leave out the effects of wind absorption entirely on the grounds that the wind optical depth in Hα is usually much less than unity. Indeed, it is true that τ(Hα) is small in all but the innermost portion of O star winds.

Here wind absorption has been accounted for (eq. [1]), and its effects are found to be significant. The reason for this is simply that the radial dependence of the wind emission is very heavily weighted in favor of the smallest radii. To demonstrate this, the radial emission profile, $r^2\epsilon(r)$, is plotted for a selection of wind models in Figure 6. The effect of wind absorption is clearly apparent in the downturn of these curves as they are followed in from large r. If absorption is left out of account, there is no downturn, and instead $r^2\epsilon(r)$ rises sharply as the photosphere is approached. In § III, where the character of the L(Hα) fits was discussed, the magnitude and the sense of the dependence of L(Hα) upon stellar radius was explained as the consequence of a competition between wind Hα optical depth and emission measure. Hence, by not taking wind absorption into account, Leitherer overestimates the effective Hα emissivity of O star winds and so finds in favor of the less massive winds produced by a more steeply accelerating velocity law.

This criticism of Leitherer's (1988) interpretation of his $\dot{M}$-L(Hα) relation does not, of course, invalidate the use of the relation to determine mass-loss rates. This is because its absolute scaling is fixed to ensure that, on average, Garmany and Conti's (1984) ultraviolet mass-loss rates are reproduced. Leitherer also showed that his fit gives mass-loss rates that are in agreement with radio determinations. This is not entirely surprising in view of Garmany and Conti's finding that the $L_{\rm bol}$-$\dot{M}$ relation defined by the ultraviolet mass-loss rates merges nicely with the radio results. Since Leitherer's Hα method gives results that agree with alternative measures of mass-loss rate, there is value in directly comparing the results of the theoretical $\dot{M}$-L(Hα) relation with his results. In particular, it is of interest to establish whether the factor of 2 discrepancy emerging from the comparison with radio mass-loss rates persists for the greater number of less luminous stars Leitherer was able to include in his sample.

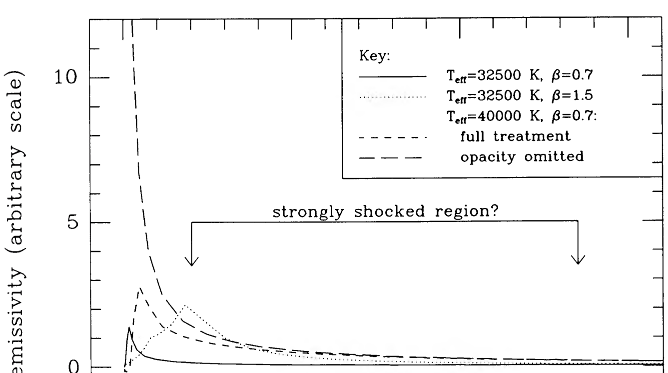

FIG. 6.—H I Hα emissivity profiles [$r^2\epsilon(r)$] calculated for some of the $T_{\rm eff}$ = 32,500 K and 40,000 K supergiant wind models (see Table 1). Ordinate units are arbitrary. For the $T_{\rm eff}$ = 40,000 K supergiant model, the emissivity profile has been calculated both in accordance with eq (1) (which allows for line opacity) and also in the optically thin approximation adopted by Leitherer (1988). The radial range within which the numerical modeling of Owocki, Castor, and Rybicki (1988) predicts the formation of strong shocks is indicated.

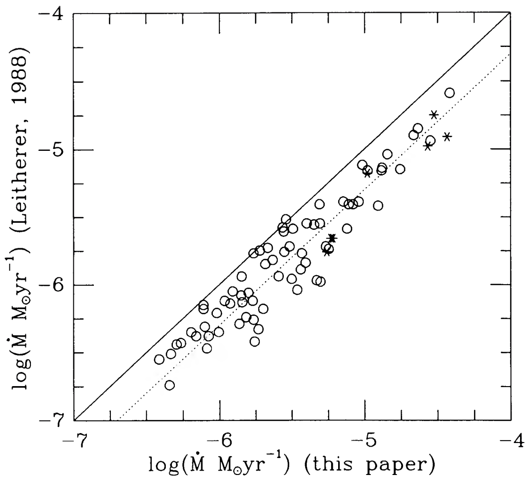

FIG. 7.—A comparison of O star mass-loss rates calculated from H I Hα measurements for a β = 0.7 velocity law (eq. [8]) and using Leitherer's (1988) fit. All the data used in the $\dot{M}$ determinations are from Table 1 of Leitherer's paper. Stars for which radio mass-loss rates are available are distinguished by the asterisks. Solid line indicates equality between the two derivations. Along the dotted line, Leitherer's mass-loss rates are half those obtained here.

Mass-loss rates derived by Leitherer (1988) and those derived from equation (8) (for β = 0.7) are plotted against each other in Figure 7. The Hα luminosities, terminal velocities, and stellar radii used in the latter fit are taken from Table 1 of Leitherer's paper. Only those stars with $L(\text{H}\alpha)/L_\odot \geq 0.1$ and O, B0, I, or B0.5 I spectral trypes are included. Clearly the theoretical $\dot{M}$-L(Hα) continues to overestimate the mass-loss rate and again the typical discrepancy is a factor of 2. There is thus little doubt that the theoretical $\dot{M}$-L(Hα) relation really does systematically underestimate the efficiency of Hα emission in O star winds.

VI. DISCUSSION

Clearly the results of the comparisons presented above can be interpreted in one of two ways: either it is supposed that the time-independent model with a much more gradual velocity law ($\beta \simeq 1.5$) than is predicted can explain the results, or else the time-independent model is regarded as unsatisfactory. Which view is the more plausible?

The gradient of the velocity law predicted by the time-dependent theory depends upon the radial dependence of the line acceleration, which in turn depends upon trends in the heavy element ionization. Our detailed understanding of the ionization of heavy elements in O star winds remains poor, primarily because of the major uncertainties of the properties of the extreme ultraviolet radiation field (see discussion by Drew 1989). Pauldrach (1987) has calculated a line-driving force that is consistent with the wind ionization structure, but this model does not include a self-consistent thermal balance calculation and also fails to fit both high- and low-ionization resonance line profiles simultaneously. Although existing wind ionization models are inadequate, it is by no means obvious that the predicted line-driving force is badly affected, given the enormous number of lines (both optically thick and thin and from many stages of ionization) that contribute to its final form (Abbott 1982). To achieve an acceleration that is sufficiently gradual to produce a $\beta \simeq 1.5$ velocity law, the effect of radial dilution of the continuum radiation field upon the line-driving force must be countered by a radial increase in the wind's specific opacity at the relevant wavelengths. Conditions in Wolf-Rayet winds might allow this, but it seems highly improbable that conditions in O star winds do. The dominant role of the dilution of the radiation field in O star winds has meant that predictions of time-independent dynamical models have all converged on relatively steeply rising velocity laws. For example, Friend and Abbott (1986) obtained $\beta \simeq 0.8$, while recent calculations by Pauldrach *et al.* (1990) suggest the range, $0.7 \lesssim \beta \lesssim 1.1$. To make matters worse, Puls (1987) has argued that a proper account of radiation trapping associated with multiple line scattering results in little change to the derived wind acceleration. In short, it would seem there is little real hope that the time-independent model can accommodate a $\beta = 1.5$ velocity law.

This returns us to the expectation that the smooth density profile of the time-steady radiative-driving model is interrupted by shocks. Is there likely to be enough postshock compression to significantly alter the effective Hα emissivity? To answer this, it is necessary first to identify where, in the time-independent case, most of the Hα emission is produced. It was shown in Figure 6 that the radius of peak Hα emission (after weighting the emissivity by r^2) lies inside $\sim 1.3R$. At larger radii, the emission falls off fairly sharply. Radiation-driven winds are expected to be most susceptible to the growth of instabilities where the outflow is both supersonic and steeply accelerating (see, for example, Owocki and Rybicki 1985). Recent numerical hydrodynamic simulations by Owocki, Castor, and Rybicki (1988) have begun to quantify this view. For the particular case they treat (a mid-O supergiant with $\dot{M} = 5.6 \times 10^{-6}\ M_{\odot}\ \mathrm{yr}^{-1}$), shock compression is most pronounced in the range $1.2 \lesssim r/R \lesssim 2.3$, where $\langle \rho^2 \rangle / \langle \rho \rangle^2$ peaks at a value of 6. Further compression occurs out to $r/R \lesssim 4$ where a typical value of $\langle \rho^2 \rangle / \langle \rho \rangle^2$ is 2. If these results are taken as representative of what is happening in O star winds, the Hα emissivity will be enhanced by factors of a few out to $r/R \leq 4$ relative to what is expected in the time-independent case. In view of the character of the radial emission profiles shown in Figure 6, it is plausible that this enhancement, particularly within $r/R \lesssim 2$, could result in the modest increase in L(Hα) that is needed to explain the over-large mass-loss rates that have been derived here (Fig. 3).

There is another independent piece of evidence that suggests O star Hα emission is affected by wind instabilities. It was pointed out by Ebbets (1982) that Hα is commonly variable in strength and that the character of the profile variations suggests a complex non-spherically symmetric source for the variability. This behavior is easily accommodated within the time-dependent radiation-driven wind model. The Hα variation observed in α Cam, ϵ, and ζ Ori amounts to about 20% of the wind equivalent width (i.e., after the photospheric contribution has been removed). For these same stars, Leitherer (1988) has adopted wind Hα equivalent widths that are at the bottom end of the range reported by Ebbets. The implications of this are that plotted positions for these stars in Figures 3 and 4 could be somewhat below their mean positions and that the resultant discrepancies between the radio and Hα mass-loss rates for $\beta = 0.7$ may be on the low side. Clearly, more Hα observations would not go amiss in properly defining the nature and extent of the variability.

It remains true that wind emission in Hα exhibits a very good correlation with wind mass-loss rate. Hence, its value as a mass-loss rate determinant is not diminished. The $\dot{M}$-L(Hα) calibration presented here can be used to obtain mass-loss rate estimates in cases where $\dot{M}$ is in excess of $\sim 10^{-6}\ M_{\odot}\ \mathrm{yr}^{-1}$. It would appear that the effect of density inhomogeneities due to shocking can be accounted for by combining the fit appropriate to a $\beta = 0.7$ velocity law (eq. [8]) with the correction given in equation (9). The recommended fit is thus:

$$\log \dot{M}_{-6} = 0.821 \log [L(\mathrm{H}\alpha)/L_{\odot}] + 1.312 \log v_{\infty,3} - 0.192 \log R - 0.437\ . \quad (10)$$

The error intrinsic to the fitting procedure alone is of the order of 20%–30%. However, when equation (10) is used to obtain a plot of $\dot{M}$ against L_{bol} for the subset of Leitherer's sample included in Figure 7, the standard deviation with respect to the mean log (L_{bol})–log $\dot{M}$ relation derived by Garmany and Conti (1984) is 0.48. This happens to be the same scatter as Garmany and Conti obtained on combining their ultraviolet $\dot{M}$ values with the radio sample, but it is rather larger than that obtained by Leitherer (1988). The origin and the significance of this scatter remains debatable.

Finally, it must be stressed that equation (10) should not be applied to B stars (other than perhaps B0 or B0.5 supergiants) or in cases where $L(\mathrm{H}\alpha)/L_{\odot} < 0.1$. However, it is an advantage of the O star fit obtained here that the dependence on photospheric parameters is so weak compared with the necessary dependences on L(Hα) and v_{∞}.

REFERENCES

Abbott, D. C. 1982, *Ap. J.*, **259**, 282.
———. 1985, in *Radio Stars*, ed. R. M. Hjellming and D. M. Gibson (New York: Plenum), p. 61.
Barlow, M. J. 1985, in *Massive Stars*, Lectures given at 4th British-Spanish School in Astrophysics, Granada, Spain.
Bieging, J. H., Abbott, D. C., and Churchwell, E. 1989, *Ap. J.*, **340**, 518.
Bertout, C., Leitherer, C., Stahl, O., and Wolf, B. 1985, *Astr. Ap.*, **144**, 87.
Cassinelli, J. P., 1985, in *The Origin of Non-Radiative Heating and Momentum in Hot Stars*, ed. A. B. Underhill and A. G. Michalitsianos (NASA/CNRS Monograph Series), p. 2.
Castor, J. I. 1970, *M.N.R.A.S.*, **149**, 111.
Drew, J. E. 1989, *Ap. J. Suppl.*, **71**, 267 (Paper I).
Ebbets, D. 1982, *Ap. J. Suppl.*, **48**, 399.
Friend, D. B., and Abbott, D. C. 1986, *Ap. J.*, **311**, 701.
Friend, D. B., and Castor, J. I. 1983, *Ap. J.*, **272**, 259.
Garmany, C. D., and Conti, P. S. 1984, *Ap. J.*, **284**, 705.
Garmany, C. D., Olson, G. L., Conti, P. S., and van Steenberg, M. E. 1981, *Ap. J.*, **250**, 660.
Klein, R. I., and Castor, J. I. 1978, *Ap. J.*, **220**, 902 (KC).
Leitherer, C. 1988, *Ap. J.*, **326**, 356.
Lucy, L. B. 1982, *Ap. J.*, **255**, 286.
Mihalas, D. 1972, NCAR Technical Note STR-76.
Owocki, S. P., Castor, J. I., and Rybicki, G. B. 1988, *Ap. J.*, **335**, 914.
Owocki, S. P., and Rybicki, G. B. 1985, *Ap. J.*, **299**, 265.

Panagia, N., and Felli, M. 1975, *Astr. Ap.*, **39**, 1.
Pauldrach, A. 1987, *Astr. Ap.*, **183**, 295.
Pauldrach, A., Kudritzki, R. P., Puls, J., and Butler, K. 1990, *Astr. Ap.*, **228**, 125.
Pauldrach, A., Puls, J., and Kudritzki, R. P. 1986, *Astr. Ap.*, **164**, 86.
Puls, J. 1987, *Astr. Ap.*, **184**, 227.
Snow, T. P., and Morton, D. C. 1976, *Ap. J. Suppl.*, **32**, 429.
Walborn, N. R. 1982, *Ap. J.*, **256**, 452.
Wright, A. E., and Barlow, M. J. 1975, *M.N.R.A.S.*, **170**, 41.

J. E. DREW: Department of Astrophysics, Nuclear Physics Laboratory, Keble Road, Oxford, OX1 3RH, England, UK